Accepted Manuscript

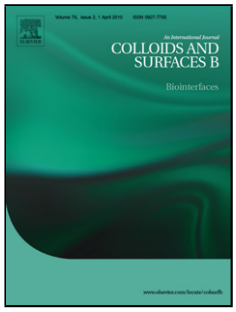

Title: Protonation of β-lactoglobulin <!–<query id="Q1">Please check the presentation of dochead Ẅull length article, and correct if necessary.</query>–>in the presence of strong polyelectrolyte chains: A study using Monte Carlo simulation

Authors: Paola Torres, Luciano Bojanich, Fabricio Sanchez Varreti, Antonio Jose Ramirez-Pastor, Evelina Quiroga, Valeria Boeris, Claudio F. Narambuena

PII: S0927-7765(17)30593-3
DOI: http://dx.doi.org/10.1016/j.colsurfb.2017.09.018
Reference: COLSUB 8837

To appear in: *Colloids and Surfaces B: Biointerfaces*

Received date: 11-6-2017
Revised date: 29-8-2017
Accepted date: 6-9-2017

Please cite this article as: {http://dx.doi.org/

Protonation of β-lactoglobulin in the presence of strong polyelectrolyte chains: a study using Monte Carlo simulation.

Paola Torres[¶,£], *Luciano Bojanich*[§], *Fabricio Sanchez Varreti*[£], *Antonio Jose Ramirez-Pastor*[¶], *Evelina Quiroga*[‡], *Valeria Boeris*[§,†], *and Claudio F. Narambuena*[¶,£,*]

[¶]Instituto de Física Aplicada, Universidad Nacional de San Luis-CONICET. San Luis, Argentina.

[§]Universidad Nacional de Rosario - CONICET. Facultad de Ciencias Bioquímicas y Farmacéuticas. Área Fisicoquímica. Rosario, Santa Fe, Argentina.

[£]Universidad Tecnológica Nacional, Facultad Regional San Rafael, Mendoza, Argentina

[‡]Laboratorio de Membranas y Biomateriales. Instituto de Física Aplicada, Universidad Nacional de San Luis-CONICET. San Luis, Argentina.

[†]Universidad Católica Argentina. Facultad de Química e Ingeniería. Rosario, Santa Fe, Argentina.

*Corresponding author: cfnarambuena@gmail.com

Graphical Abstract

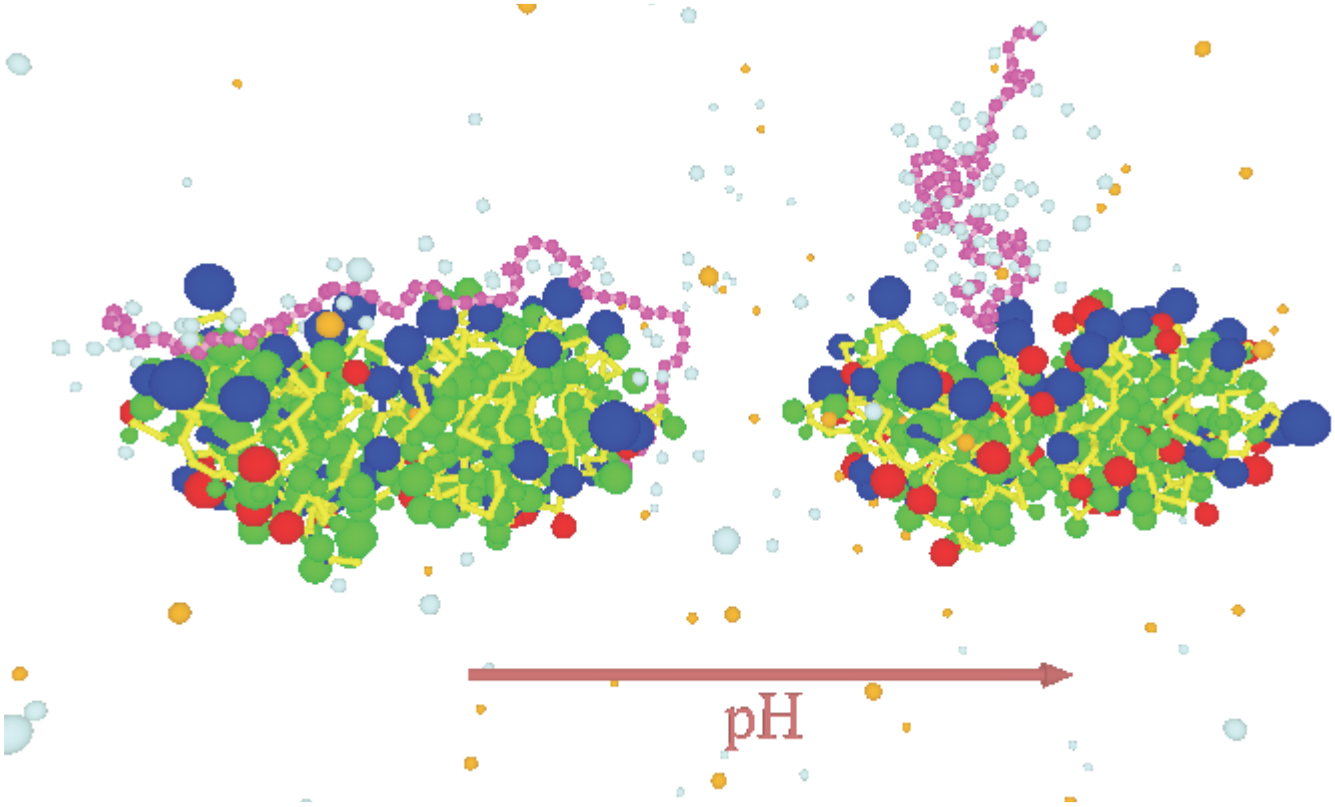

Highlights

- The molecular interaction between the β-lactoglobulin and PE chains was studied.
- Charge regulation mechanism plays a key role on BLG-PE interaction.
- The complexation on the wrong side of pH was more evident with polycation chains.
- The GLU and ASP groups play a key role in the charge reversion of the protein.
- Polyanion and polycation were spatial adsorbed in different region on the protein.

ABSTRACT

In this work, the molecular interaction between the protein β-lactoglobulin and strong polyelectrolyte chains was studied using Monte Carlo simulations. Different coarse-grained models were used to represent the system components. Both net charge and protonation of the isolated dimeric protein were analyzed as a function of pH. The acid-base equilibrium of each titratable group was distinctively modified by the presence of polyanion or polycation chains. The complexation on the wrong side of pI was more evident with the polycation than with the polyanion. It was mainly due to a charge regulation mechanism, where the reversion in net charge of the protein was more pronounced at the left of isoelectric point of the protein. The glutamic and aspartic groups play a key role in this charge reversion. Both polyanion and polycation were spatially adsorbed in different region on the protein surface, suggesting the importance of the surface charge distribution of the protein.

KEYWORDS: Whey proteins; Polyelectrolyte; β-lactoglobulin; Complex

1. Introduction

Milk whey is the remaining liquid after coagulation of the caseins during the cheese making process. High volumes of whey are generated during cheese production, representing up to 90% of the milk volume, its correct treatment being environmentally relevant.[1] Whey contains not only lactose but also $\sim 8\, g/L$ proteins, mainly β-lactoglobulin and α-lactalbumin. Whey proteins (WP) have been intensively studied due to their nutritional and functional importance as a food additive.[2,3] These proteins are concentrated from whey usually by means membrane technologies.[4,5] However, this methodology is not accessible to small industries due to the need of continuous processes and to a the high cost of the

membranes. Accordingly, the precipitation of the proteins using polyelectrolytes (PE) is a simple, quick and cheap method which can be applied at an industrial scale.[6]

Numerous experimental studies have focused on the interaction between proteins and PE.[7,8] Several intermolecular interactions are involved; yet, electrostatic attraction is often the main responsible of protein-PE interactions, taking place in two steps:[7-9] i) interaction between the electrical charges of PE and the opposite electrical charges of the protein, forming a complex between one PE chain and several protein molecules; ii) interaction between soluble complexes leading to non-soluble particles (of high molecular mass), which is evident by the phase separation of the system. This second step may be monitored by turbidimetry. The resulting complexes may be easily separated by decantation[8] and can be applied as a food additive, requiring the use of a food-grade PE, such as polysaccharides like alginate, chitosan.

Complex coacervation and precipitation of WP with different PE were reported.[10,11] The fractionation of different WP was also carried out by precipitation with carboxymethylcellulose.[12] In addition, functional properties of mixed systems composed of WP and PE were also reported.[13,14] Harnsilawat et al. studied the interaction between β-lactoglobulin (BLG) and alginate.[15] However, the experimental conditions required to produce the effective interaction of the proteins with a PE are usually determined empirically and involves many assays varying pH, concentration of each polymer and ionic strength. Theoretical studies may improve the understanding of these systems and the design of purification processes. In addition, the number of experimental assays may be reduced if factors affecting protein-PE interaction are well known.

Carlsson et al. studied the electrostatic interaction between lysozyme and a flexible chain of PE using Monte Carlo (MC) simulation.[16] The protein was represented by a coarse-

grained model consisting of a hard sphere with embedded discrete charges. The authors found that an additional attractive short-range potential between the protein and polyelectrolyte bead was need to obtain complexation when both species had similar net charge. On the other hand, the electrostatic complexation of flexible anionic PE with whey proteins was studied by Vries using MC simulation at their respective isoelectric point (pI).[17] The author found that the attractive interaction between α-lactalbumin and PE was stronger than BLG-PE interaction. This behavior was explained considering the differential superficial charge distribution of each protein: there is a localized positively charged "patch" in α-lactalbumin, responsible for binding the PE, while multiple smaller charge patches are found in BLG, which explain the weaker complexation. However, in these works the fluctuating nature of the acid-base equilibrium of the titratable groups of the protein was neglected. However, Barroso da Silva & Jönsson[18] studied the complexation of several proteins, including BLG and α-lactalbumin, with PE using MC simulations. In this case the representation of protein was more sophisticated, since the protein was modeled as a rigid body in full atomistic detail. The authors took into account the acid-base equilibrium of protein, allowing titratable groups to change their charge state according to electrostatic environment and solution pH. They found that the charge regulation mechanism was responsible for the attractive forces between the protein and the PE when the pH was "on the wrong side" of the isoelectric point.

The complexation, aggregation and precipitation of protein-PE systems are process with different spatial-temporal scales that are still not completely understood. This can be separated into a small and a big spatial scale: on the small scale the molecular interaction between the protein and PE plays a major role, in particular, the electrostatic interaction between their charged groups. These interactions and spatial distribution of charged groups modulate the acid-base equilibrium of titratable groups, which originate the complex

formation between a PE chain and several protein molecules. On the big scale, it is important to consider the interaction between complexes to form the insoluble aggregates.

In this work we focus on the molecular-level interaction between BLG and PE. The balance between electrostatic interactions and the acid-base equilibrium of titratable groups was studied to determine how the charge of each type of protein residue is affected by the presence of PE chain. Thus, the main objective of this work was to study the acid-base equilibrium of each type of titratable group in the presence of both, a strong anionic and a strong cationic PE.

This article is structured around the following sections: Section 2, called "Computational Methods", describes coarse-grained models and Monte Carlo methodologies. Section 3 reports and discusses the results found. Section 4 provides conclusions and broader perspectives.

2. Computational Methods

The present study was carried out using MC simulation, taking into account that: i) two protein chains (forming a dimer) were localized in the center of a cubic simulation box of $L \times L \times L$ size, with periodic boundary conditions in all three directions; ii) the volume and temperature were constant in the simulation; iii) in the initial configuration, a PE chain could or could not be added to the system; iv) the number of molecules of the protein and PE was fixed along the simulation; and v) there was an explicit representation of small ions originated from the added salt and from the ionization of the protein and PE.

Different coarse-grained models were used to represent the small ions, PE chain and protein molecule.

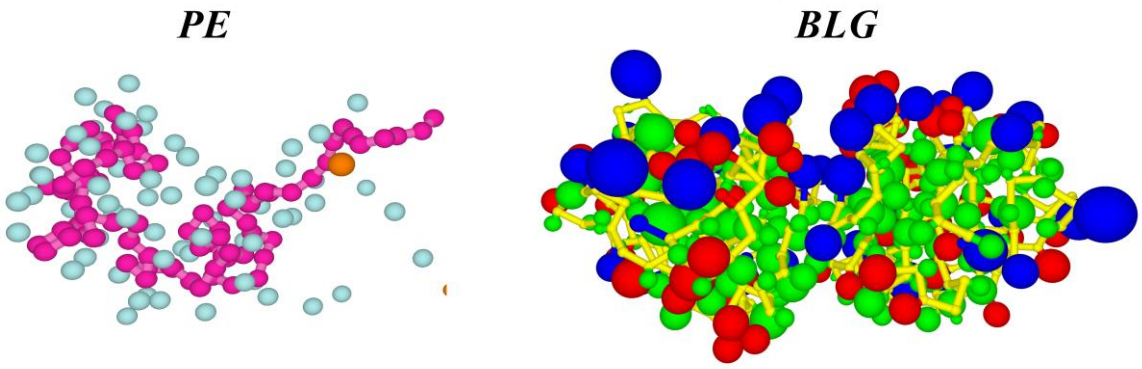

Figure 1. Coarse-grained model for PE and dimeric BLG. Anionic PE is depicted in pink with its counterion atmosphere formed by small cations (turquoise); small anions (orange) are also depicted. The protein titratable groups are depicted full charged, positive (blue) and negative (red). The non-titratables or neutral groups are shown in green. The principal backbone is depicted with yellow cylinders and α-carbons in yellow spheres.

Figure 1 shows the different coarse-grained models used to represent the small ions, PE and BLG. The solvent (water) was modeled in terms of an implicit solvent with a relative dielectric constant $\varepsilon_r = 78$. The small ions were monovalent, cations and anions corresponding to Na^+ and Cl^- ions, respectively. The small ions are represented by rigid spheres of diameter $d = 0.4\,nm$, with a monovalent charge embedded in the center of the sphere.

The PE chain was made up from a group of charged beads (or monomers) bound forming a lineal chain.[19] Each bead was represented as a rigid sphere (diameter $d = 0.2$ nm) with the corresponding electrical charge embedded in the center (Figure 1). The energetic connectivity of two consecutive beads, i and $i+1$ (localized at positions r_i and r_{i+1} respectively), was represented by an harmonic bond potential given by:

$$U_{bond} = k_{bond}(l - l_0)^2 \quad (1)$$

where $l = |r_{i+1} - r_i|$ is the distance between two consecutives beads, and $l_0 = 0.25\,nm$ is the equilibrium bond length. The bond stiffness is regulated by k_{bond}, which is the spring force constant for the potential in Equation 1. In order to avoid fluctuations in bond length a high value of this constant, $k_{bond} = 1000\,k_bT/nm$, was chosen. In this work, the energy units are normalized to the thermal energy k_bT, where k_b is the Bolztmann constant and T is the absolute temperature ($T = 300\,K$).

The electrostatic potential energy of the system composed of N total charged particles (residues, bead of PE and small ions) was modeled as the sum of coulombic interaction pairs:

$$\frac{U_{elect}}{k_bT} = l_B \sum_{i=1}^{N-1} \sum_{j=i+1}^{N} \frac{z_i z_j}{r_{ij}} \quad (2)$$

where the charge q_i of the particle can be expressed as $q_i = ez_i$, e being is the elemental charge and z_i the valence. The distance between the particles is $r_{ij} = |r_j - r_i|$ and l_B is the Bjerrum length having the form:

$$l_B = \frac{e^2}{4\pi\varepsilon_r\varepsilon_0 k_bT} \quad (3)$$

where ε_0 is vacuum dielectric constant. At room temperature in water the Bjerrum length has a value of $l_B \approx 0.71nm$.

In a previous work we found that the stiffness of this polyelectrolyte model can be characterized by two persistence lengths, which depends on the intrinsic flexibility of the chain and the electrostatic interactions.[20] In the present work we choose an intrinsic full flexible chain characterized by an intrinsic persistence length of $l_p^0 \cong 0.2\,nm$ and an electrostatic persistence lengths $l_p^e \cong 20\,nm$, which quantify the chain stiffness due to electrostatic interactions.

The experimental data of the protein structure were obtained from x-ray structure hosted in the Protein Data Bank (1BEB for β-lactoglobulin).[21] The coarse-grained model used in this work was built from the position of each atom that comprises the protein. Each aminoacid was represented by two beads, one for the α-carbon and the other for the residue of the aminoacid. At each end of the protein chain there are free functional groups, which can be of amino or carboxylic nature. These groups were denominated N terminal ($N-ter$) or C terminal ($C-ter$), respectively. An additional bead represented each terminal group.

The structure of a polypeptide chain is characterized by the positions of the α-carbons. Each α-carbon was approached by rigid spheres of diameter $d = 0.2\ nm$. These α-carbons built the protein backbone (yellow spheres and cylinder in the Figure 1). In turn, each α-carbon was connected to a side chain or residue, called R group, that set the nature of each amino acid. Each R group comprised a group of atoms (between the atoms n_i and n_f) and was represented by a single rigid sphere used to approach the corresponding excluded volume. The position and radius of each rigid sphere was calculated using the protein x-ray structure, described in detail in section 1 (SI1) of supplementary information (SI). In order to simplify the simulated system, the dimeric form of the BLG was considered to be predominant in the conditions studied.

There are two general types of residues regarding their acid-base capacity: neutral and titratable. Neutral R groups do not have capacity for ionization and are only characterized by their excluded volume. The titratable residues are classified into acid (Asp, Glu, Cys, Tyr) or basic (Arg, His, Lys) and each one is characterized by an intrinsic acid-base constant K_{ai} value, shown in Table 1.[22] The number of each titratable group in the dimer of BLG (ω_i) is also shown in Table 1.

Table 1. pK_a value and amount of each titratable group ω_i present in BLG dimer.

	Asp	Glu	Cys	Tyr	$C-ter$	Arg	His	Lys	$N-ter$
pK_{ai}	4.0	4.4	9.5	9.6	3.8	12.0	6.3	10.4	7.5
ω_i	20	32	2	8	2	6	4	30	2

In ideal conditions, where each group does not interact with the others, the dissociation degree for each type of acid and basic titratable group is:

$$\theta_{Ai} = \frac{1}{1+10^{(pK_{ai}-pH)}} \quad (4)$$

$$\theta_{Bi} = \frac{1}{1+10^{(pK_{ai}-pH)}} \quad (5)$$

The charge contribution of each type of acid and basic group is defined as $Z_{Gi} = -\omega_i\theta_{Ai}$ and $Z_{Gi} = \omega_i(1-\theta_{Bi})$ respectively. The ideal net charge of the protein molecule can be calculated as:

$$Z_{BLG} = -\sum_{i=1}^{5}\omega_i\theta_{Ai} + \sum_{i=6}^{9}\omega_i(1-\theta_{Bi}) \quad (6)$$

where the first and second term of equation represent the charge contribution due to the five types of acid and four types of basic groups, respectively. Equation 6 is deduced in detail in supplementary information.

This theoretical scheme describes the acid-base equilibrium of titratable groups taking into account exclusively the intrinsic pK_a and pH values. However, the electrostatic environment where the group is localized can affect its dissociation degree. This electrostatic effect was included in the titration scheme of the MC method used in this work.[23-26]

2.1. Simulation method

In order to evaluate the structural properties, the Metropolis Monte Carlo (MC) algorithm was used in a system with a constant temperature and volume.[27] In the initial

configuration, the protein, PE and small ions were randomly positioned inside the simulation box. Since each particle was represented as a hard sphere, overlapping was avoided. In order to equilibrate the system, the translational motion of small ions, the PE chain (with its condensed ionic atmosphere), was considered. The protein molecule was considered a rigid body, and the configurational movements were not allowed. However, the PE chain was configurationally relaxed means pivot and flip motions to reach the system equilibrium.[19] Movements were accepted according to the probability:

$$min\{1, exp(-\Delta U_{el}/k_B T)\} \qquad (7)$$

where ΔU_{el} represents the change of electrostatic energy between the initial and final states.

The protonation state of titratable groups was modified using a MC semigrancanonical procedure described in detail in SI (Section SI3) and in cited references.[28-31] During the protonation (deprotonation) procedure the charge was increased (decreased) by +1 due to proton binding (unbinding) to the group. Therefore, the creation (deletion) of a small anion was required in order to maintain the electroneutrality of the system. The probability of accepting the protonation (deprotonation) trail is:

$$min\left(1, e^{-\beta\Delta U_{el} \pm (pH - pK_a) ln10}\right) \qquad (8)$$

where the sign $-$ or $+$ is corresponds to protonation or deprotonation respectively. The net charge of a BLG dimer and the partial charge contributions (due to each type of titratable groups) were calculated as ensemble averages.

Then, the system had a constant number of protein molecules, volume and temperature (NVT), which is a canonical ensemble for the protein dimer. However, for the titration of acid-base equilibrium, a semi-grand canonical ensemble was used, since the protonation or deprotonation of titratable groups was associated with the creation or deletion

of small anions. Ionic strength in the system was maintained using a MC scheme in the grand canonical ensemble, where salt concentration was treated with an algorithm of insertion or deletion of neutral pairs of salt particles. This algorithm matched the chemical potential of salt in the system with the value in reservoirs.[32] In this work, the corresponding salt concentration in reservoirs was $c_{Salt} = 10mM$. The side size of simulation box was $L = 20nm$, therefore, the final concentration of the protein and polyeletrolyte was $C_{Prot} \cong 0.4\,mM$ and $C_{PE} \cong 0.2\,mM$ respectively. The concentration of the protein was twice the concentration of polyelectrolyte, since we assumed that the protein exists in its dimeric form.

3. Results and discussion

This work addresses the PE adsorption on the BLG and the effect of this interaction on the acid-base equilibrium of protein residues. The titration equilibrium of the isolated protein in solution was first studied. Then, the interaction of the protein with anionic and cationic strong PE was analyzed.

3.1. Protonation behavior of isolated BLG in solution.

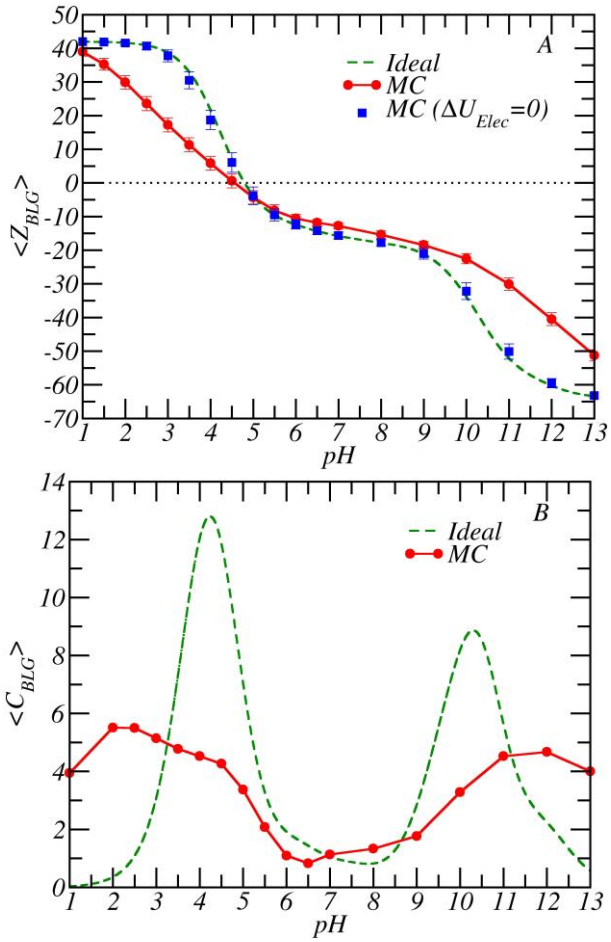

Figure 2. Protonation behaviour of isolated BLG. (A) Protein net charge as a function of pH solution and (B) protein capacitance as a function of pH solution, both obtained from Monte Carlo simulation (symbol) at $c_{Salt} = 10mM$. The ideal titration curve (Equation 6) and capacitance (Equation 9) is also depicted for comparison purposes.

The net charge of the BLG as a function of pH is shown in Fig. 2A. The MC results at salt concentration equal to $c_{Salt} = 10mM$ (red filled circles) are depicted together with the ideal curve (green dashed line) obtained from Equation 6. At acidic conditions the BLG was positively charged. The maximum $Z_p \cong 40$ observed at extreme acidic conditions was close to the total number of basic groups (Table 1). This maximum value was achievable thanks to the full protonation of the titratable groups in BLG dimer, making that all basic groups are charged and all acid groups are neutralized. The BLG net charge decreased as the solution

pH value increased. The isoelectric point of BLG was estimated around 4.6 from the extrapolation in simulated curve of Figure 2A. Experimental value of pI is approximately 5.1 depending on the type and concentration of salt used.[33-35] The simulated curve has a minimum of $Z_p \cong -50$ at $pH = 13$. This charge value does not match with the total amount of acid groups of the protein (64 acid groups for BLG dimer). The difference may be attributed to a combination of partial ionization of acidic and basic groups or to the full deprotonation of acidic groups and a partial protonation of basic groups.

The ideal net charge of the protein displayed a similar trend to that shown by the simulated net charge (Fig. 2A). The agreement between the simulated and the ideal titration curve is acceptable in a moderate pH range ($4 < pH < 9$). At strong acidic ($pH < 3$) and basic ($pH > 9$) conditions, the net charge of the BLG obtained by simulation shows a lower absolute value in comparison to that obtained by the ideal curve, calculated by assuming that there were no intramolecular interactions between residues. It is known that the electrostatic environment could affect the acid-base equilibrium of each titratable group. This was taken into account in the MC simulation, since an electrostatic energetic term ΔU_{el} was included in the acceptance probability of protonation (Eq. 8). When the MC simulation was carried out with the protonation process without including the electrostatic contribution: $\Delta U_{el} = 0$, the resulting curve (blue square) was in excellent agreement with the theoretical one.

The ability of the protein to change its net charge in terms of the electrostatic environment is called charge regulation and is quantified by capacitance:[30]

$$C_{BLG} = \langle Z_{BLG}^2 \rangle - \langle Z_{BLG} \rangle^2 = \frac{1}{\ln 10} \frac{\partial Z_{BLG}}{\partial pH} \qquad (9)$$

Figure 2B depicts the BLG capacitance as a function of pH. This profile has two peaks (localized at low and high pH values) and a valley at moderate pH values. The first

peak is in the pH range $2-5$, which ends close to the isoelectric point of the protein. The second peak starts at pH above 9. Below we analyze the contribution of each titratable group type to the net charge (Fig. 3) and the effect on BLG capacitance.

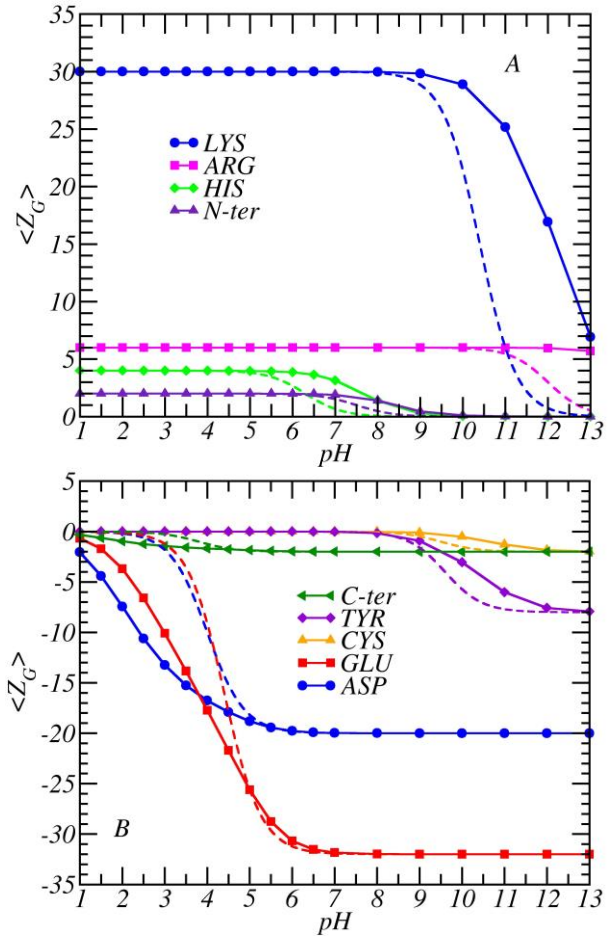

Figure 3. Partial charges contribution due to (A) basic and (B) acidic residues of BLG as a function of pH solution obtained from MC simulation (symbols and continuous lines) at $c_{Salt} = 10mM$. The ideal titration curve is depicted for comparison (dashed lines).

The partial charges of basic and acidic groups as a function of solution pH are shown in Figure 3 (A) and (B) respectively. The MC results are represented in symbols and the ideal curve in dashed lines.

The basic groups were fully charged (protonated) at low pH values, matching with the corresponding ideal values for each group (Fig. 3A). These values agree with the amount of each titratable group (ω_i) in BLG dimer (Table 1). As pH increased, the deprotonation of these groups began. The MC protonation results of these groups maintained a high protonation degree compared to the ideal value, i.e., the simulated titration of these groups were shifted to the right compared to ideal values.

In order to understand this behavior, the case of histidines will be explained in detail. The four histidine residues (intrinsic $pka = 6.3$) had a shift at high pH values with the order of a pH unit (Fig. 3A). The histidine groups were the presence of the net negative charge due to the remaining charged groups of the BLG, since in these conditions, the pH solution was beyond the pI (Fig. 2A). Then, the protonation trial of histidine consists in change of their neutral initial state to a positively charged final state. The new positive charge electrostatilly interacts (Eq. 2) with the remaining charges of the BLG, with net negative charge. The sum of new coulombic terms is negative (since the new positive charge is electrostatically attracted for the negative charge of BLG) and, therefore, the final (protonate) state has a lower electrostatic energy than the neutral initial state. This allows histidine groups to have a negative value in the electrostatic energy change for their protonation trial: $\Delta U_{el} < 0$. This increases the probability of protonation, which is proportional to $e^{-\beta \Delta U_{el} - (pH - pK_a) ln10}$. Therefore, these residues have an effective pka that shifts to the right of their intrinsic pka value. For the lysine and arginine groups, the magnitude of the shift is higher, around two pH units, since, in this condition, the BLG has a much more negative charge (Fig. 2A) hence, ΔU_{el} for protonation has a much more negative value. This leads to a deep protonation shift of lysine and arginine groups at high pH values. In turn, this shift is the main responsible for the variation of the simulated protein net charge in relation to the ideal value (Fig. 2A) with a minor contribution due to the low ionization of TYR and CYS groups (Fig. 3B).

The ionization of acidic groups is also affected by the net charge of the protein (Fig. 3B). Cysteine and tyrosine are less negatively charged (more protonated) than the ideal one at high pH values. In this range the protein has a net negative charge, generating an electrostatic repulsion on the charged state of cysteine or tyrosine; i.e., it is easier to protonate these groups. Therefore, the ionization of these acidic groups is weaker than that in the ideal one at high pH values.

At high pH values the acidic groups tend to be more protonated than the ideal one, at low pH values they are more deprotonated. As pH decreases below the pI, the protein has a positive net charge. Then, the deprotonate state of acid group (negatively charged) has a lower electrostatic energy than that of the protonate state (neutral state). For example, aspartic and glutamic groups are much more negatively charge than the ideal one.

The total net charge environment of the protein contributes to the protonation or deprotonation process at high or low pH values, respectively. While at acid pH values the shift between the simulated and ideal curve is to the left (more deprotonated), in basic pH values this shift is to the right (more protonated).

3.2. Interaction of BLG and a strong PE chain

Figure 1 shows a typical frame of protein and an anionic PE chain in conditions of $pH = 7$ and $c_{Salt} = 10mM$. Under these conditions, the PE chain is far from the protein and surrounded by an atmosphere of condensed counterion. Since the equilibrium bond length (l_0) is lower than the Bjerrum length l_B, an amount of condensed small cations can be found on the PE chain; this phenomenon is called Manning condensation.[36]

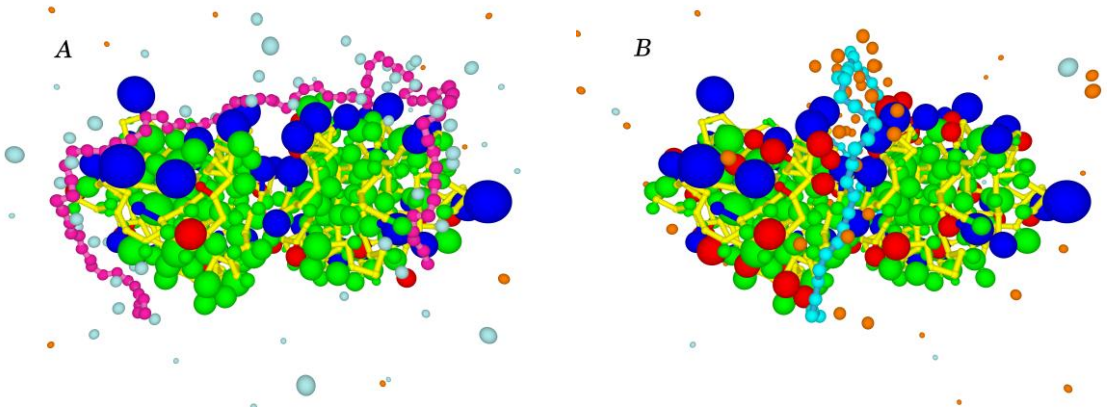

Figure 4. Typical frames obtained from Monte Carlo simulation of complex BLG-PE, for A) Polyanion and B) Polycation. In both cases the polyelectrolytes are fully flexible chains with $N_m = 80$ and $l_0 = 0.25\ nm$. The solution has $pH = 4$ and $c_{Salt} = 10mM$.

The typical frames obtained by MC simulation at $pH = 4$ of the BLG form complex with polyanion and polycation (both with $N_m = 80$ and $l_0 = 0.25\ nm$) are shown in Figure 4, panel A and B respectively. More frames can be found in two animations stored as supplementary information.

In these figures we observe the presence of positively charged patches on the protein surface; the basic groups remain fully charged on this pH value. The distribution of this positive charge patch is parallel to the axis connecting the monomers of BLG. The anionic PE chain is localized mainly parallel to this axis (Fig. 4A). Then a positive patch guides the spatial distribution of the polyanion on the protein surface. However, the polycation is adsorbed perpendicularly to the axis that connects the two protein molecules. In this region of the protein surface, a negatively charged patch is formed (Fig. 4B).

In both cases the amount of small ion adsorbed on the PE chain (counterion condensation) remained significant, although the PE was adsorbed on the protein surface.

The BLG-PE interaction is molecularly quantified throughout a simple structural criterion, which calculates the number of monomers of PE chain that are in close contact with the titratable groups of the protein. The distance of separation Δr between the centre of each monomer and each titratable residue was measured. Adsorbed monomers (θ) denote the number of monomers within a distance shorter than $\Delta r < r_C$, where $r_C = 0.5\, nm$ is the cut radius. This simple criterion of distance with was used to quantify the counterion condensation on PE chain, in excellent agreement with experimental results.[19] This adsorption criterion is discussed in detail in the supplementary information (S4).

BLG has weak titratable groups which can be in neutral or charged state depending on envioronmental conditions. PE has strong dissociated groups, then its monomer are fully charged in all conditions. Each monomer of polyacid experiences an electrostic attraction by positively charged groups (protonated basic groups) of BLG. Therefore, the number of ionic pairs may be calculated as the amount of adsorbed monomer on titratable groups that are positively charged $\theta_P = \langle n_P \rangle$, where n_P is the number of monomer adsorbed on a positevely charged titratable groups. Similarly, when the PE is cationic, the number of monomers close to negatively charged groups is calculated, $\theta_N = \langle n_N \rangle$. The brackets denote an ensemble average.

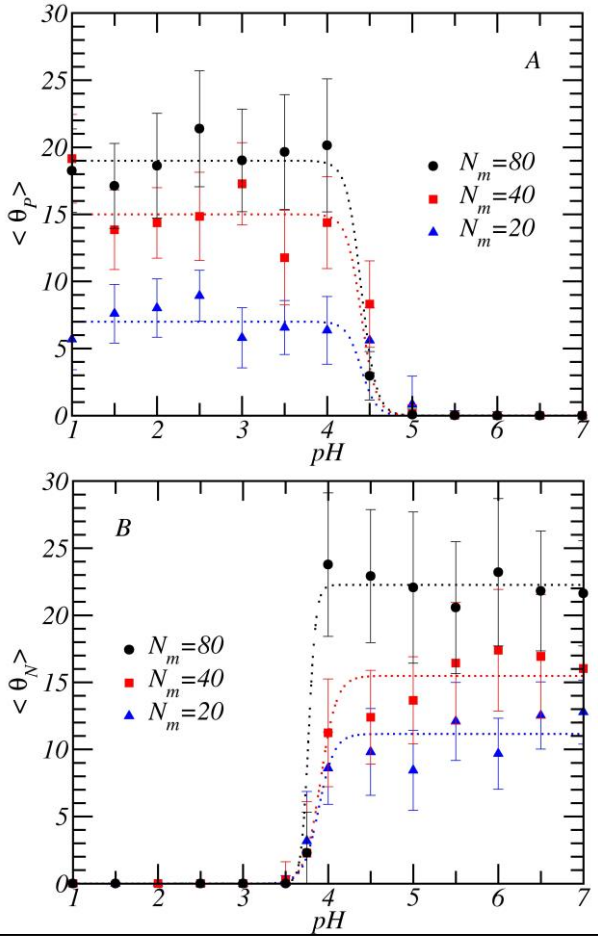

Figure 5. Number of monomers adsorbed on the oppositely charged residues as a function of pH at different chain sizes and $c_{Salt} = 10mM$. A) Polyanion-BLG. B) Polycation-BLG. Dotted lines only serve the purpose of guiding the eyes.

Figure 5 shows monomer adsorption on the oppositely charged group of BLG as a function of pH. Figure 5A shows monomers adsorption on basic charged titratable group at different chain sizes of the polyanion. At pH values above the isoelectric point, there are no monomer adsorbed near the protein. This can be attributed to a repulsive interaction between the BLG and PE, since both macromolecules have negative charge. Monomer adsorption took place at pH values lower than $pH = 5$, close to the protein isoelectric point. The amount of adsorbed monomers increased quickly as the solution pH decreased. However, at pH lower than $pH = 4$, the amount of adsorbed monomers remained in a value approximately constant. However, when chain size was small, the amount of monomers adsorbed increased

lineally (approximately half monomers of the PE chain). When the amount of adsorbed monomers was larger, it reached a plateau. This indicates that the BLG dimer has a limited capacity to bind monomers of the PE chain. We can infer which of these monomers form ionic pairs, the maximum of ionic pairs is close to $\theta_P \approx 20$ for the longer PE (80 monomers per chain).

Harnsilawat et al. have studied the interaction between BLG and alginate (an anionic polysaccharide) and have experimentally quantified the maximum amount of alginate bind to BLG at different values of pH using ITC.[15] At $pH = 3$, the interaction between $0.1\ wt\%$ of BLG and alginate is exothermic up to $\sim 0.9\ \mu M$ of sodium alginate. Based on the experimental values[15] and considering the dimeric form for BLG it is estimated that there are about 27 protein molecules for each alginate chain. The relationship between the amount of alginate monomers by each protein molecule is also estimated. This would indicate the presence of approximately 39 monomers of alginate for each protein molecule forming the complex. Figure 5A suggests that for the longest anionic chain ($N_m = 80$) are 20 monomers that electrostatic interacts with positively charged groups of protein. These monomers are not consecutives, and there are others that do not form ionic pairs. Considering both cases then the total amount of adsorbed monomer on the protein are approximately 30. In the real system several protein molecules attractively interact with the polyelectrolyte chain. Then the experimental value take into account both the adsorbed monomers (forming or not ionic pairs) and the monomers that form the linkers between complexes formed for a protein molecule and a portion of the PE chain.

The interaction between strong cationic PE and BLG was quantified by the monomer adsorption θ_N on negatively charged groups showed in Figure 5B. At low pH values, monomer adsorption on the protein was negligible, since the two molecules were positively

charged, leading to an electrostatic repulsion between them. The θ_N on the protein started to be significant at acid values $pH \approx 4.0$ and quickly reached a plateau. The amount of monomers adsorbed on the protein surface monotonically increased as the size of the PE chain increased. For the longest chain, a saturation of adsorbed monomers on the protein was reached.

Monomer adsorption on the protein begins at pH values lower than the isoelectric point of isolated protein where apparently both, protein and PE, have positive charge. This formation of complex "on the wrong side" of the isoelectric point has been studied for several authors.[9,17,37,38] Two main molecular interpretations have been formulated for this phenomenon. The first one assumes the existence of charged patches on the BLG surface[9,17,37,38] and the second takes into account the charge fluctuations that allow modifying the net charge of the protein through the charge regulation mechanism.[39-42]

It was previously suggested that the presence of anionic or cationic PE chain could modify the net charge of the protein below the isoelectric point by a charge regulation mechanism. Then the question is how monomer adsorption affects protein net charge.

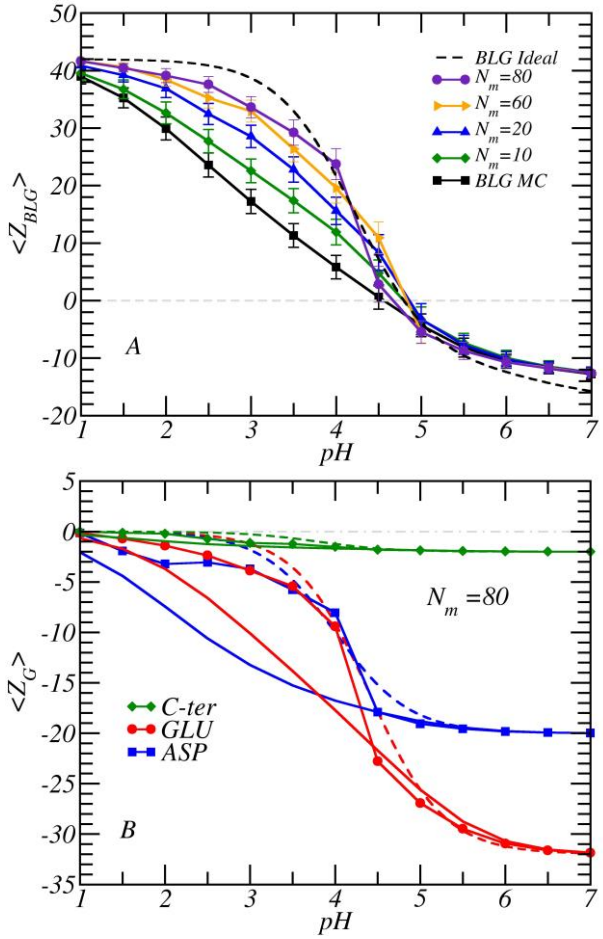

Figure 6. A) Protein net charge as a function of pH, in the presence of a polyelectrolyte chain with different sizes N_m (symbols and continuous lines) and isolated protein (continuous line). B) Partial charge due to acid groups ($C-ter$, GLU, ASP) of the protein as a function of pH solution obtained from the Monte Carlo simulation. Symbol with continue lines depict the interaction between the protein and an anionic PE ($N_m = 80$). The acidic groups of isolated protein are depicted in continuous lines. For both figures the ideal titration curve is depicted in dashed lines and $c_{Salt} = 10mM$.

Figure 6 depicts the protein net charge as a function of solution pH in the presence of the anionic PE. The size of the PE chain (N_m) has a minimum of 10 and a maximum of 80 monomers, which are fully charged throughout the entire pH range studied.

At low pH values the protein molecule has positive net charge that originates an attractive electrostatic interaction with the PE. This is indirectly observed by the increment of the positive net charge of the protein below pI. The increase in the size of the PE chain amplifies the effect on the protein net charge. As a result the protein net charge at a pH value is higher for the longest chain and the curve is pushed closer to the ideal one.

At high pH values the protein has a negative net charge, causing an electrostatic repulsion with PE. This can be inferred from Figure 6 since the net charge of the protein in the presence of PE becomes similar to the simulated curve of the isolated protein above the isoelectric point.

The protein net charge in the presence of the longest anionic PE studied ($N_m = 80$) is around 20 positive charges higher than in the isolated protein at $pH = 3.5$. The basic titratable groups are fully charged at low pH values even with the presence of the anionic PE (data shown in SI5). Figure 6B shows the partial charge of acidic titratable groups: $C-ter$, GLU, and ASP (continuous lines with symbols) when interacting with the anionic PE ($N_m = 80$). Figure 6B also shows the ideal (dashed lines) and the simulated isolated protein (continuous line) curve for the acidic groups studied. It should be noted that the charge contribution of Cys and Tyr groups are not shown in Figure 6B. This is due to their pK_a values that are higher than 9.0; then in the pH range studies are fully protonated and do not change their charged state in the presence of the anionic PE chain.

The $C-ter$, GLU, and ASP groups are much more negatively charged (more deprotonated) in simulated isolated protein than in the ideal conditions. However, in the simulation of the protein in the presence of an anionic PE chain, intensifies the protonation process of the glutamic and aspartic group compared to the isolated protein (Figure 6B). Thus, the negative charge of GLU and ASP groups is neutralized. Then, the partial charge

contribution of these groups in the presence of the PE becomes very similar to those under ideal conditions.

The GLU and ASP groups are the main responsible for the increase in protein net charge ($\sim$20 positive charges) in the presence of PE at $pH = 3.5$ (Fig. 6A). Each group losses around 10 negative charges (after the interaction with the PE chain) which accounts for the consequent increase in the protein net charge.

The interaction of protein molecule with a strong cationic PE is analyzed below.

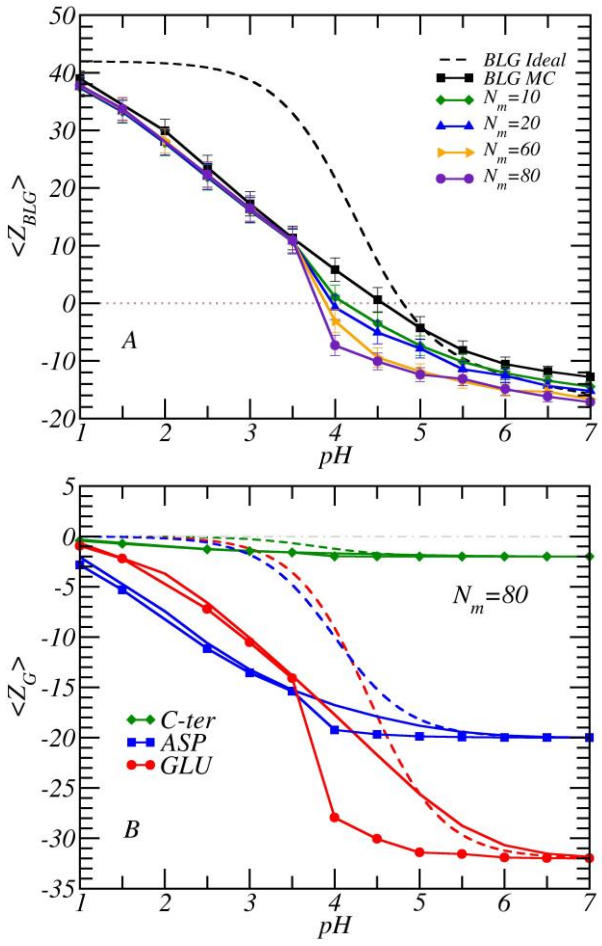

Figure 7. Cationic polyelectrolyte chain effects on the ionization of protein. A) BLG net charge as a function of pH at different chain sizes and $c_{Salt} = 10mM$. B) Partial charge due to acidic groups of protein as a function of pH solution obtained from MC simulation. Continuous lines with symbol depict the interaction of the protein with the cationic PE ($N_m = 80$) and $c_{Salt} = 10mM$. The titratable groups of isolated protein are depicted in continuous lines. The ideal titration curve is depicted in dashed lines.

Figure 7A presents the polycation chain size effect on the protein net charge as a function of the pH. The curves obtained from the MC simulation of isolated protein were also depicted. At low pH range ($pH < 3.5$) the protein net charge in the presence of the cationic PE is slightly smaller than that the corresponding to the isolated BLG profile. However, at $pH > 3.75$ the protein net charge strongly decreases in such a way that it becomes negative. This net charge reversion of BLG occurred with monomer adsorption on the protein (Fig. 5B). Indeed, this protein capacity to change its net charge explains the formation of BLG-PE complex on the wrong side of the isoelectric point. Then, the protein that forms part of the complex has an effective isoelectric point that is lower than the pI value of isolated protein. As the PE chain size increases, the effective pI of the protein shifts to lower values. The protein net charge becomed much more negative as the PE chain size increases, in agreement with the amount of monomer adsorbed on the protein. At $pH = 4$ the difference between the protein net charge forming BLG-PE complex ($N_m = 80$) and isolated protein is approximately 16 units (Fig. 7A). The titratable groups that play key roles in this variation of the protein net charge were studied.

The protonation behavior of the acidic groups in the presence of the cationic PE ($N_m = 80$) is represented as a function of pH in Figure 7B (the results of MC simulation of the isolated protein are also shown). The ionization change is notable in the acid range 3 <

$pH < 6$, the presence of polycation especially intensifies the ionization of glutamic acid. The formation of complex at $pH = 4$ proceeds with deprotonation of approximately 10 glutamic residues; therefore, the protein added approximately 10 negative charges. However, the change in the protein net charge at $pH = 4$ is approximately 16 units (Fig. 7A). Then the glutamic groups are the main responsible for the charge reversion on the protein.

4. Conclusions:

The molecular interaction of β-lactoglobulin with a strong PE chain was studied using MC method. In order to study the acid-base equilibrium of titratable groups of the protein, a semi-grand canonical scheme was used. This allowed studying the protein in isolated conditions and in interaction with strong polyanion or polycation. Both PE chains are structurally identical (fully flexible with equal l_0 value); the key difference lies in the electrostatic charge sign of their monomers.

The isoelectric point value of isolated BLG obtained from MC simulation was consistent with the experimental value. The polyanion was adsorbed on the protein surface from extreme acid until pH values close to the protein isoelectric point. However, the polycation adsorption on the protein starts at pH values lower than the pI (the wrong side complexation) and persists at higher pH values. In both cases, the presence of PE modified the net charge of protein. This charge regulation is more evident at pH values lower than the pI, where the capacitance of protein shows a maximum, since an important number of acid groups (mainly glutamic and aspartic) with pKa values can be found in this range. The general effect is that the isoelectric point of the BLG shifts to the right approximately one quarter of pH unit by the presence of polyanion, and it shifts to the left in approximately one pH unit interacting with the longest chain of polycation.

Then, this work predicts that in the interaction of BLG with a polyanion or polycation, the charge regulation mechanism plays a key role. In addition, with PEs of similar structural characteristics (fully flexible and strong charged), the phenomenon of complex formation "on the wrong side" is more evident with the polycation than with a polyanion.

This work has two immediate perspectives: i) it establishes the conditions of chain size, pH and c_{Salt} for the complexation of several BLG molecules with a single PE chain; ii) it helps understanding the interaction of a PE chain with monomeric or multimeric forms of BLG and the competition with other whey proteins, such as α-lactalbumin or lactoferrin.

ACKNOWLEDGMENT

E.Q. thanks support from Universidad Nacional de San Luis (Argentina) under project 2-2116. A.J. R-P. thanks support from Universidad Nacional de San Luis (Argentina) under project 03-0816; CONICET (Argentina) under project PIP 112-201101-00615; and the Agencia Nacional de Promoción Científica y Tecnológica (Argentina) under project PICT-2013-1678. L.B. and V.B. thanks support from Secretaría de Políticas Universitarias under project "Jorge Sábato". L.B., V.B. and C.F.N. thanks support Universidad Nacional de Rosario under project 1BIO495. The language assistance by Andrea Torres and Carolina Mosconi is gratefully acknowledged.

REFERENCES

(1) Prazeres, A. R.; Carvalho, F.; Rivas, J. *J Environ Manage* **2012**, *110*, 48.
(2) Suárez, A.; Fernández, L.; Balbarie, P.; Iglesias, J. R.; Riera, F. A. *European Food Research and Technology* **2016**, *242*, 1211.
(3) Livney, Y. D. *Current Opinion in Colloid & Interface Science* **2010**, *15*, 73.
(4) Jeewanthi, R. K.; Lee, N. K.; Paik, H. D. *Korean J Food Sci Anim Resour* **2015**, *35*, 350.
(5) Marella, C.; Muthukumarappan, K.; Metzger, L. E. *J Dairy Sci* **2011**, *94*, 1165.

(6) Picó, G. A.; Woitovich Valetti, N. In *Polyelectrolytes: Thermodynamics and Rheology*; P. M, V., Bayraktar, O., Picó, G. A., Eds.; Springer International Publishing: Cham, 2014, p 245.

(7) Cooper, C. L.; Dubin, P. L.; Kayitmazer, A. B.; Turksen, S. *Current Opinion in Colloid & Interface Science* **2005**, *10*, 52.

(8) Kayitmazer, A. B.; Seeman, D.; Minsky, B. B.; Dubin, P. L.; Xu, Y. *Soft Matter* **2013**, *9*, 2553.

(9) Seyrek, E.; Dubin, P. L.; Tribet, C.; Gamble, E. A. *Biomacromolecules* **2003**, *4*, 273.

(10) Weinbreck, F.; de Vries, R.; Schrooyen, P.; de Kruif, C. G. *Biomacromolecules* **2003**, *4*, 293.

(11) Weinbreck, F.; Nieuwenhuijse, H.; Robijn, G. W.; De Kruif, C. G. *J Agric Food Chem* **2004**, *52*, 3550.

(12) Capitani, C.; Pérez, O. E.; Pacheco, B.; Teresa, M.; Pilosof, A. M. R. *Food Hydrocolloids* **2007**, *21*, 1344.

(13) Benichou, A.; Aserin, A.; Lutz, R.; Garti, N. *Food Hydrocolloids* **2007**, *21*, 379.

(14) Bédié, G. K.; Turgeon, S. L.; Makhlouf, J. *Food Hydrocolloids* **2008**, *22*, 836.

(15) Harnsilawat, T.; Pongsawatmanit, R.; McClements, D. J. *Food Hydrocolloids* **2006**, *20*, 577.

(16) Carlsson, F.; Linse, P.; Malmsten, M. *The Journal of Physical Chemistry B* **2001**, *105*, 9040.

(17) de Vries, R. *J Chem Phys* **2004**, *120*, 3475.

(18) da Silva, F. L. B.; Jonsson, B. *Soft Matter* **2009**, *5*, 2862.

(19) Narambuena, C. F.; Leiva, E. P. M. In *Polyelectrolytes: Thermodynamics and Rheology*; P. M, V., Bayraktar, O., Picó, G. A., Eds.; Springer International Publishing: Cham, 2014, p 349.

(20) Narambuena, C. F.; Leiva, E. P. M.; Chávez-Páez, M.; Pérez, E. *Polymer* **2010**, *51*, 3293.

(21) Brownlow, S.; Cabral, J. H. M.; Cooper, R.; Flower, D. R.; Yewdall, S. J.; Polikarpov, I.; North, A. C. T.; Sawyer, L. *Structure* **1997**, *5*, 481.

(22) Nozaki, Y.; Tanford, C. In *Methods in Enzymology*; Academic Press: 1967; Vol. Volume 11, p 715.

(23) Labbez, C.; Jönsson, B.; Skarba, M.; Borkovec, M. *Langmuir* **2009**, *25*, 7209.

(24) Ullner, M.; Jönsson, B. *Macromolecules* **1996**, *29*, 6645.

(25) Kesvatera, T.; Jönsson, B.; Thulin, E.; Linse, S. *Journal of Molecular Biology* **1996**, *259*, 828.

(26) Persson, B. A.; Lund, M. *Physical Chemistry Chemical Physics* **2009**, *11*, 8879.

(27) Metropolis, N.; Rosenbluth, A. W.; Rosenbluth, M. N.; Teller, A. H.; Teller, E. *The Journal of Chemical Physics* **1953**, *21*, 1087.

(28) Lund, M.; Jonsson, B. *Biochemistry* **2005**, *44*, 5722.

(29) Hyltegren, K.; Nylander, T.; Lund, M.; Skepö, M. *Journal of Colloid and Interface Science* **2016**, *467*, 280.

(30) Lund, M.; Jonsson, B. *Q Rev Biophys* **2013**, *46*, 265.

(31) Teixeira, A. A.; Lund, M.; da Silva, F. L. *J Chem Theory Comput* **2010**, *6*, 3259.

(32) Valleau, J. P.; Cohen, L. K. *The Journal of Chemical Physics* **1980**, *72*, 5935.

(33) Bromley, E. H. C.; Krebs, M. R. H.; Donald, A. M. *Faraday Discussions* **2005**, *128*, 13.

(34) Das, K. P.; Kinsella, J. E. *Journal of Dispersion Science and Technology* **1989**, *10*, 77.

(35) Sawyer, L.; Kontopidis, G. *Biochimica et Biophysica Acta (BBA) - Protein Structure and Molecular Enzymology* **2000**, *1482*, 136.

(36) Manning, G. S. *Journal of Chemical Physics* **1969**, *51*, 924.

(37) de Kruif, C. G.; Weinbreck, F.; de Vries, R. *Current Opinion in Colloid & Interface Science* **2004**, *9*, 340.

(38) Hattori, T.; Hallberg, R.; Dubin, P. L. *Langmuir* **2000**, *16*, 9738.

(39) Biesheuvel, P. M.; Wittemann, A. *The Journal of Physical Chemistry B* **2005**, *109*, 4209.

(40) da Silva, F. L. B.; Lund, M.; Jönsson, B.; Åkesson, T. *The Journal of Physical Chemistry B* **2006**, *110*, 4459.

(41) de Vos, W. M.; Leermakers, F. A. M.; de Keizer, A.; Cohen Stuart, M. A.; Kleijn, J. M. *Langmuir* **2010**, *26*, 249.

(42) Narambuena, C. F.; Longo, G. S.; Szleifer, I. *Soft Matter* **2015**, *11*, 6669.